THERMAL MODELING AND BENCHMARKING OF CRYSTALLINE LASER AMPLIFIERS*

D. T. Abell, D. L. Bruhwiler, P. Moeller, R. Nagler, B. Nash, I. V. Pogorelov
RadiaSoft LLC, Boulder, CO, USA
Q. Chen, C. G. R. Geddes, C. Tóth, J. van Tilborg, LBNL, Berkeley, CA, USA
N. B. Goldring, STATE33 Inc., Portland, OR, USA

Abstract

Ti:sapphire crystals constitute the lasing medium of a class of lasers valued for their wide tunability and ultra-short, ultra-high intensity pulses. When operated at high power and high repetition rate (1 kHz), such lasers experience multiple effects that can degrade performance. In particular, thermal gradients induce a spatial variation in the index of refraction, hence thermal lensing [1]. Using the open-source finite-element code FEniCS [2], we solve the relevant partial differential equations to obtain a quantitative measure of the disruptive effects of thermal gradients on beam quality. We present thermal simulations of a pump laser illuminating a Ti:sapphire crystal. From these simulations we identify the radial variation in the refractive index, and hence the extent of thermal lensing. In addition, we present analytic models used to estimate the effect of thermal gradients on beam quality. This work generalizes to other types of crystal amplifiers.

INTRODUCTION

Titanium-doped sapphire (Ti:sapphire) crystals constitute the lasing medium of a class of lasers valued for their wide tunability and capacity to produce ultra-short, ultra-high intensity pulses. But when operating at high power with a high repetition rate (1 to 10s of kHz), multiple natural/thermal/mechanical effects can degrade the performance of Ti:sapphire crystal laser amplifiers.

For example, during steady-state operation, *i.e.* with a crystal amplifier operating in equilibrium, thermal gradients induce both a positional variation in the index of refraction and mechanical stresses. The changes in the index of refraction can lead to thermal lensing. And stresses in an anisotropic, uniaxial crystal such as Ti:sapphire can modify the crystal's birefringent characteristics and further degrade the beam.

THERMAL MODELS AND TIME SCALES

The heat equation derives from conservation of energy and the Fourier law. In the context of heat flow in a solid, one may express conservation of energy in the form

$$\rho \frac{\partial u}{\partial t} = -\nabla \cdot \vec{q} + f, \tag{1}$$

where ρ denotes the mass density of the solid, u the internal energy per unit mass, $\vec{q}$ the local heat flux, and f a source term that represents the rate of external heat deposition per unit volume. This equation expresses the rate of change of the local energy density as a sum of the local heat loss, $-\nabla \cdot \vec{q}$, and the local heat deposition, f. The Fourier law,

$$\vec{q} = -K_c \nabla \Theta, \tag{2}$$

describes the local heat flux as proportional to and in the direction opposite the local temperature gradient, $\nabla \Theta$, with the proportionality given by K_c, the thermal conductivity. One may relate energy density and temperature via the *specific heat*, $c_p = \partial u / \partial \Theta$. This relation allows one to write

$$\dot{u} = \frac{\partial u}{\partial \Theta} \frac{\partial \Theta}{\partial t} = c_p \dot{\Theta}, \text{ and } \nabla u = \frac{\partial u}{\partial \Theta} \nabla \Theta = c_p \nabla \Theta. \tag{3}$$

In the very simplest case—ρ, K_c, and c_p experience negligible variation over the temperature range of interest—one may use the above results to derive the linear heat equation:

$$\dot{\Theta} = \frac{K_c}{\rho c_p} \nabla^2 \Theta + \frac{f}{\rho c_p} = \alpha \nabla^2 \Theta + g, \tag{4a}$$

where α denotes the *thermal diffusivity*, $K_c/(\rho c_p)$, and $g = f/(\rho c_p)$. More generally, however, the quantities K_c and c_p—and, to a much smaller extent, ρ—do vary with temperature; and one cannot then convert the heat deposition term f to a "temperature deposition" term so simply as dividing by ρc_p. In this case it simplifies matters to work with u in preference to Θ. If we may treat ρ as constant, then we instead derive the heat equation in the nonlinear form [3]

$$\dot{u} = \nabla \cdot (\alpha(u) \nabla u) + f/\rho. \tag{4b}$$

When necessary, one may convert between u and Θ by means of the (monotonically increasing) specific heat capacity.

Time Scales for Thermal Relaxation

For now we focus on the linear form Eq. (4a) of the heat equation. If the source term vanishes—except for possibly a brief pulse that defines the initial condition—and we assume azimuthal symmetry, one may use separation of variables to identify the essential functional form of the solution:

$$J_0(\nu r)[\cos(kz) + \beta \sin(kz)]e^{-\alpha(\nu^2+k^2)t}. \tag{5}$$

A complete solution, written as a linear combination of these functions, is determined by the boundary conditions, with

the system geometry constraining the possible eigenvalues ν and k.

We consider a crystal of radius a and length l with its temperature held at the fixed value Θ_D on its cylindrical boundary, and unconstrained on the end caps at $z = 0, l$. As thermal conduction is orders of magnitude faster than convection or radiation, we make the approximation that no heat flows out the end caps. As a consequence of the given constraints and geometry, the sine terms vanish, and one may write the crystal's temperature difference from the boundary in the Fourier-Bessel series form [4]

$$\Delta\Theta(r,z;t) = \sum_{n=1}^{\infty}\sum_{m=0}^{\infty}\Theta_{nm}J_0\left(\tfrac{\nu_{0n}r}{a}\right)\cos\left(\tfrac{m\pi z}{l}\right)e^{-t/\tau_{nm}},$$

(6)

where each component nm experiences its own decay rate

$$\tau_{nm}^{-1} = \alpha\left[\left(\tfrac{\nu_{0n}}{a}\right)^2 + \left(\tfrac{m\pi}{l}\right)^2\right].$$

(7a)

Here ν_{0n} denotes the nth root of J_0. The dominant time-scale is that of the lowest-order mode:

$$\tau_{10} = \frac{a^2}{\nu_{01}^2\,\alpha},$$

(7b)

which we note depends only on the crystal geometry and the thermal diffusivity.

Equilibrium Temperature Profile

To solve Eq. (4a) for the equilibrium temperature profile in the presence of a steady, azimuthally symmetric heat source $g(r,z)$, we (i) set $\dot{\Theta}$ to zero; (ii) expand both temperature, Θ, and heat source, g, as Fourier Bessel series (*cf.* Eq. (6) with no time dependence); and (iii) equate coefficients as determined by Eq. (4a). Given a source term of the form

$$g(r,z) = g_0\,g_\perp(r)\,g_\parallel(z) = \frac{f_0}{\rho c_p}\,e^{-(r/\sigma)^2}e^{-(z-z_0)/\zeta},$$

(8)

we obtain the equilibrium temperature profile in the form

$$\Delta\Theta(r,z) = \Theta_0\sum_{n=1}^{\infty}\sum_{m=0}^{\infty}R_n Z_m X_{nm}J_0\left(\tfrac{\nu_{0n}r}{a}\right)\cos\left(\tfrac{m\pi z}{l}\right).$$

(9a)

Here

$$R_n = \frac{2}{[\nu_{0n}J_1(\nu_{0n})]^2}\int_0^{\nu_{0n}}x\exp\left[-\left(\frac{ax}{\nu_{0n}\sigma}\right)^2\right]J_0(x)\,\mathrm{d}x,$$

(9b)

$$Z_m = \frac{2}{1+\delta_{m0}}\frac{l/\zeta}{(l/\zeta)^2+(m\pi)^2}\left[1-(-1)^m e^{-l/\zeta}\right],$$

(9c)

$$X_{nm} = \frac{l/a}{(\nu_{0n}l/a)^2+(m\pi)^2}.$$

(9d)

And then, with absorbed power $P_{\text{abs}} = \int f\mathrm{d}^3\vec{r} = f_0 V_{\text{eff}}$,

$$\Theta_0 = \frac{P_{\text{abs}}}{4\pi K_c}\frac{V_{\text{cyl}}}{V_{\text{eff}}},$$

(9e)

where V_{eff} denotes the *effective volume* into which the source deposits heat. The R_n denote Fourier-Bessel coefficients of the transverse source profile $g_\perp(r)$; the Z_m Fourier coefficients of the longitudinal source profile $g_\parallel(z)$; and the X_{nm} "cross-terms" that arise from the matching constraints implied by the linear heat equation Eq. (4a).

LONGITUDINAL ABSORPTION OF GAUSSIAN BEAMS

To test our understanding and benchmark our simulations, we simulate the experimental conditions of a particular Ti:sapphire crystal under study at the BELLA lab: a cylindrical crystal of length 2.5 cm and diameter 1.0 cm. A pump laser with Gaussian beam profile of width $\sigma = 0.115\,\text{cm}$ and absorption coefficient $\zeta^{-1} = 1.2\,\text{cm}^{-1}$ illuminates the entrance face of the crystal, $z_0 = -1.25\,\text{cm}$, along the cylindrical axis. Because heat deposition decays exponentially as the beam traverses the crystal, we use the heat load Eq. (8) with temperature "deposition rate" and effective volume given by

$$\mathrm{d}T = g_0 = \frac{f_0}{\rho c_p} = \frac{P_{\text{abs}}}{\rho c_p V_{\text{eff}}},$$

(10)

$$V_{\text{eff}} = \pi\sigma^2\zeta(1-e^{-l/\zeta}).$$

(11)

Using the open-source, finite-element PDE solver FEniCS [2], we simulated this system and obtained both qualitative and quantitative agreement with the above theory: The system equilibrates to a temperature distribution matching that given in Eq. (9); and, after turning off the source, we see the temperature decay exponentially to Θ_D with a thermal decay time matching that in Eq. (7b). Figure 1 shows a series of transverse and longitudinal temperature profiles computed by FEniCS during the approach to thermal equilibrium.

Quantitative agreement with experiment, however, has proved challenging: Either the decay constant Eq. (7b), the maximum on-axis temperature, $\Theta(0,0)$, or both, can differ significantly from that measured experimentally. This challenge derives from uncertainties in our knowledge of the thermal and optical properties of Ti:sapphire. We discuss this in the conclusions.

NEAR-AXIS INDEX OF REFRACTION

A principal motivation for our thermal simulations is a desire to better understand thermal lensing, wherein thermally induced variations in the index of refraction across the crystal can focus the laser wavefront [5].

Because the refractive index varies approximately linearly with temperature, $n(\Theta) = n_0 + n_T(\Theta - \Theta_D)$ [6], and the near-axis temperature varies approximately quadratically with radius (see Fig. 1), the near-axis refractive index varies approximately quadratically with radius: $n(r) = n_0 + n_2 r^2$. On the basis of data extracted from our thermal simulation, we thereby compute near-axis profiles for the coefficients n_0 and n_2. See Fig. 2.

Closely related results appear in a companion paper [7].

CONCLUSIONS AND FUTURE WORK

On the basis of the crystal geometry, $r = 0.5\,\text{cm}$, and the experimentally measured thermal time scale of c.150 ms, we compute from Eq. (7b) a thermal diffusivity α of about $0.288\,\text{cm}^2/\text{s}$. Moreover, simulations using this value of α exhibit the expected 150 ms decay time. However, tabulated
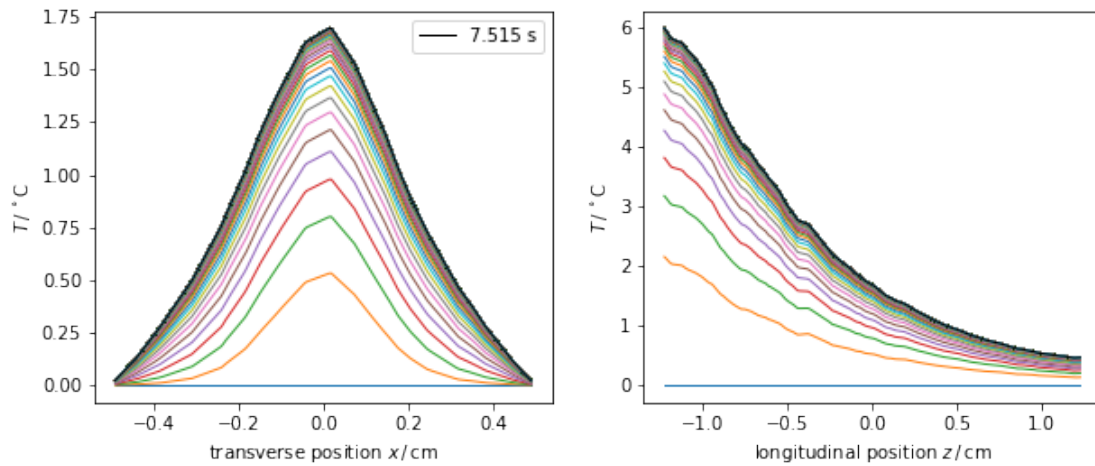
Figure 1: Transverse temperature profiles (left) at the crystal center ($z = 0$ cm) and longitudinal profiles along the crystal axis ($r = 0$ cm). The individual profiles show convergence towards thermal equilibrium in time steps of 15 ms.
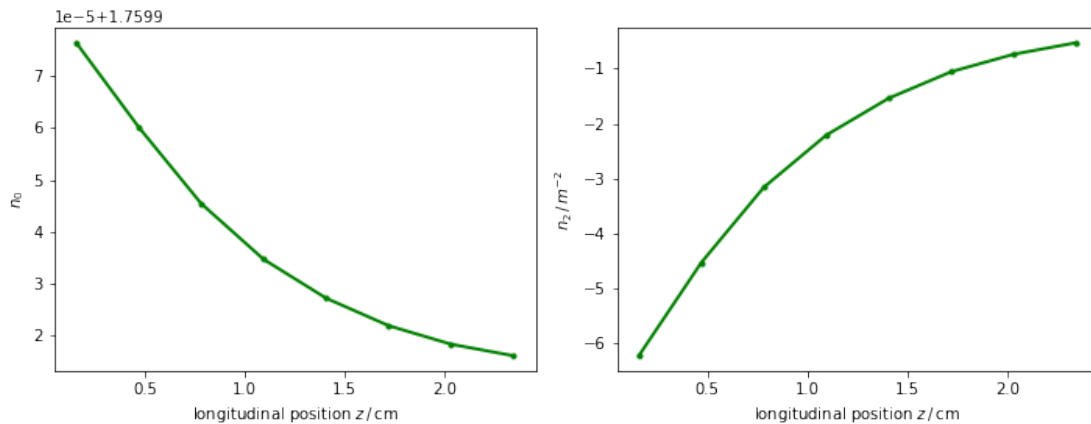

Figure 2: These graphics show the coefficients n_0 (left) and n_2 (right) that describe the temperature-induced radial variation in the near-axis refractive index: $n(r) = n_0 + n_2 r^2$.

values of the thermal properties of sapphire [8, 9] lead, *cf.* Eq. (4a), to values several times smaller: $\alpha \approx 0.1$ cm^2/s. On the other hand, data sheets specific to Ti:sapphire[1] lead to a very wide range of values: 0.06 cm^2/s to 0.31 cm^2/s. (We assume the mass density of Ti:sapphire differs little from that of sapphire: $\rho = 3.98$ gm/cm^3.)

Apart from geometric factors, the temperature increase at the center of the crystal's entrance face depends, *cf.* Eqs. (9e) and (11), on the ratio of absorbed power P_{abs} to the product of absorption length ζ times thermal conductivity K_c. See also [10]. A measurement of that temperature increase therefore implies (given the known crystal geometry) a value for that ratio. Then, given a measured temperature increase of about 7 °C, and inferring experimental values for P_{abs} and ζ, we thereby compute for K_c a value of about 0.31 W/(cmK), close to that quoted in the literature for sapphire, and well within the range quoted for Ti:sapphire.

Finally, using our derived values for α and K_c, we may compute for the specific heat capacity c_p a value of about

0.267 J/(gmK). This value is of order half that of values quoted for Ti:sapphire.

A number of uncertainties lead to this state of affairs: Perhaps most significant is the actual power absorbed as heat by the crystal: Not only is the absorption coefficient ζ^{-1} uncertain, so is the *fractional thermal heat load* η, which describes the fraction of pump laser energy absorbed as heat.

Our principal lessons here are that we require a better understanding of the actual laser power that is absorbed as heat, and also of the corresponding absorption length. In addition, we require a better understanding of both thermal conductivity and specific heat capacity in the crystalline laser gain media—especially the extent to which Ti doping modifies those parameters. This information is essential for accurate simulations going forward.

Future work will focus on three areas: (i) Improve our understanding of the thermal and optical properties of Ti:sapphire crystals. (ii) Use physically realistic wavefronts for our thermal source terms. (iii) Compare experimental measurements of thermal lensing against expectations derived from curves such as those in Fig. 2.

---

[1] See, for example, `https://www.advatech-uk.co.uk/ti_sapphire.html` and `http://singlecrystal.eu/html/ti_sapphire.html`.

REFERENCES

[1] S. Cho, J. Jeong, S. Hwang, and T. J. Yu, "Thermal lens effect model of Ti:sapphire for use in high-power laser amplifiers," *Applied Physics Express*, vol. 11, no. 9, p. 092 701, 2018, `doi:10.7567/apex.11.092701`

[2] *FEniCS*, https://fenicsproject.org/.

[3] M. A. Rincon, J. Limaco, and I.-S. Liu, "A nonlinear heat equation with temperature-dependent parameters," *Math. Phys. Electron. J.*, vol. 12, no. 5, 2006, `http://www.maia.ub.es/mpej/Vol/12/5.pdf`

[4] J. D. Jackson, *Classical Electrodynamics*, Third. John Wiley & Sons, 1999.

[5] J. Jeong, S. Cho, S. Hwang, B. Lee, and T. J. Yu, "Modeling and analysis of high-power Ti:sapphire laser amplifiers — A review," *Appl. Sci.*, vol. 9, p. 2396, 2019, `doi:10.3390/app9122396`

[6] J. Tapping and M. L. Reilly, "Index of refraction of sapphire between 24 and 1060 °C for wavelengths of 633 and 799 nm," *J. Opt. Soc. Amer. A*, vol. 3, no. 5, pp. 610–616, 1986, `doi:10.1364/JOSAA.3.000610`

[7] D. L. Bruhwiler *et al.*, "Open Source Software to Simulate Ti:Sapphire Amplifiers," presented at IPAC'22, Bangkok, Thailand, Jun. 2022, paper THPOTK063, this conference.

[8] D. A. Ditmars, S. Ishihara, S. S. Chang, G. Bernstein, and E. D. West, "Enthalpy and heat-capacity standard reference material: Synthetic sapphire (α-Al$_2$O$_3$) from 10 to 2250 K," *J. Res. Natl. Bur. Stand.*, vol. 87, no. 2, pp. 159–163, 1982, `doi:10.6028/jres.087.012`

[9] E. R. Dobrovinskaya, L. A. Lytvynov, and V. Pishchik, "Properties of sapphire," in *Sapphire: Material, Manufacturing, Applications*, 2009, pp. 55–176, `doi:10.1007/978-0-387-85695-7_2`

[10] M. E. Innocenzi, H. T. Yura, C. L. Fincher, and R. A. Fields, "Thermal modeling of continuous-wave end-pumped solid-state lasers," *Appl. Phys. Lett.*, vol. 56, no. 19, pp. 1831–1833, 1990, `doi:10.1063/1.103083`